MOLECULAR AND CELLULAR BIOLOGY, Sept. 2011, p. 3630–3638 Vol. 31, No. 17
0270-7306/11/$12.00 doi:10.1128/MCB.01462-10
Copyright © 2011, American Society for Microbiology. All Rights Reserved.

# Slowly Progressing Nucleotide Excision Repair in Trichothiodystrophy Group A Patient Fibroblasts[▽]

Arjan F. Theil,[1] Julie Nonnekens,[1,2,3] Nils Wijgers,[1] Wim Vermeulen,[1]* and Giuseppina Giglia-Mari[1,2,3]*

*Department of Genetics, Erasmus MC, Molewaterplein 50, 3015 GE Rotterdam, The Netherlands[1]; CNRS, Institut de Pharmacologie et de Biologie Structurale, 205 route de Narbonne, F-31077 Toulouse, France[2]; and Université de Toulouse, UPS, IPBS, F-31077 Toulouse, France[3]*

Received 22 December 2010/Returned for modification 9 February 2011/Accepted 15 June 2011

**Trichothiodystrophy (TTD) is a rare autosomal premature-ageing and neuroectodermal disease. The photohypersensitive form of TTD is caused by inherited mutations in three of the 10 subunits of the basal transcription factor TFIIH. TFIIH is an essential transcription initiation factor that is also pivotal for nucleotide excision repair (NER). Photosensitive TTD is explained by deficient NER, dedicated to removing UV-induced DNA lesions. TTD group A (TTD-A) patients carry mutations in the smallest TFIIH subunit, TTDA, which is an 8-kDa protein that dynamically interacts with TFIIH. TTD-A patients display a relatively mild TTD phenotype, and TTD-A primary fibroblasts exhibit moderate UV sensitivity despite a rather low level of UV-induced unscheduled DNA synthesis (UDS). To investigate the rationale of this seeming discrepancy, we studied the repair kinetics and the binding kinetics of TFIIH downstream NER factors to damaged sites in TTD-A cells. Our results show that TTD-A cells do repair UV lesions, although with reduced efficiency, and that the binding of downstream NER factors on damaged DNA is not completely abolished but only retarded. We conclude that in TTD-A cells repair is not fully compromised but only delayed, and we present a model that explains the relatively mild photosensitive phenotype observed in TTD-A patients.**

DNA lesions that disturb proper Watson-Crick base pairing are targets for the nucleotide excision repair (NER) pathway (32). NER is a versatile DNA repair system able to recognize and remove a large variety of DNA lesions, including the major UV light-induced photoproducts cyclobutane pyrimidine dimers (CPD) and 6-4 pyrimidine-pyrimidone photoproducts (6-4PPs). The biological importance of NER is illustrated by the severe clinical consequences associated with hereditary photohypersensitive NER deficiency disorders: the cancer-prone syndrome xeroderma pigmentosum (XP [MIM 278700-780]) and the neurodevelopmental conditions Cockayne syndrome (CS [MIM 214150]) and trichothiodystrophy (TTD [MIM 601675]) (2, 26).

NER is a highly coordinated multistep process initiated by two lesion recognition pathways: transcription-coupled NER (TC-NER) and global genome NER (GG-NER) (14, 21). TC-NER is initiated by lesions located in the transcribed strand of active genes that stall elongating RNA polymerase II (RNAP2); CSB (Cockayne syndrome B protein) senses stalled RNAP2 and recruits the preincision NER factors (15). Damage recognition of lesions located anywhere in the genome by GG-NER is achieved by the concerted action of the XPC-RAD23B-Cen2 and UV-damaged DNA-binding protein (UV-DDB) complexes (43). After initial damage recognition, these two subpathways funnel into a common process that involves the opening of the DNA helix by the helicase function of the basal transcription factor II H (TFIIH) (44, 57). Subsequently, TFIIH (28), together with XPA (xeroderma pigmentosum group A), verifies the lesion (44) and with RPA (replication protein A) properly orients the two structure-specific endonucleases XPG (xeroderma pigmentosum group G) (33, 61) and ERCC1-XPF complex (for excision repair cross-complementing protein 1 and xeroderma pigmentosum group F protein) (38) (responsible for the 3′ and 5′ incisions, respectively). The highly coordinated dual incision of XPG and ERCC1-XPF (39) excises a stretch of 27 to 29 nucleotides containing the lesion. The resulting single-strand gap is filled in by DNA replication proteins (34) and sealed by DNA ligases (30).

The central NER factor TFIIH is a multifunctional complex that plays a fundamental role in opening the helix of DNA around the lesion and setting the stage for the incision of the damaged strand (44). Initially, TFIIH was isolated as a general transcription factor (GTF) (8), though this multisubunit complex displays several functions, including ribosomal transcription, activated transcription, and cell cycle control (9, 62).

TFIIH is composed of 10 proteins (17): seven subunits (XPB, XPD, p62, p52, p44, p34, and TTDA) form the core complex, and three subunits (CDK7, MAT1, and CCNH) form the TFIIH-associated cyclin-activating kinase (CAK) subcomplex. The CAK complex is linked to the core via interactions with the XPD subunit (46) and plays a role in the phosphorylation of the C-terminal domain (CTD) of RNAP2 (23) and in cell cycle control (13). The two DNA-dependent helicases XPB and XPD catalyze DNA unwinding, which is required for both RNAP2 promoter escape and the DNA repair reaction (10, 20, 46).

Most likely because of its diverse cellular functions, mutations in TFIIH subunits (XPB, XPD, and TTDA) are associated with a surprisingly heterogeneous panel of phenotypes

* Corresponding author. Mailing address: Department of Genetics, Erasmus MC, Molewaterplein 50, 3015 GE Rotterdam, The Netherlands. Phone for Wim Vermeulen: 31 10 70 43 194. Fax: 31 10 70 44 468. E-mail: w.vermeulen@erasmusmc.nl. Phone for Giuseppina Giglia-Mari: 33 5 61 17 58 54. Fax: 33 5 61 17 58 71. E-mail: ambra.mari@ipbs.fr.

▽ Published ahead of print on 5 July 2011.

(55) and include the tumorigenic XP; the nontumorigenic, neurodegenerative, and premature-ageing syndromes CS and TTD; and combined forms of these syndromes, XP-CS (24) and XP-TTD (3). Interestingly, while XP and CS phenotypes can arise from mutations in different NER-related genes, photosensitive TTD is an exclusively TFIIH-related syndrome.

TTD is a premature-ageing syndrome, with the hallmark features of brittle hair and nails, ichthyosis, and progressive mental and physical retardation (12). Within photosensitive TTD, three TFIIH-coding genes have been found to be mutated: *XPB* (58), *XPD* (4, 42), and *TTDA* (17).

TTDA is an 8-kDa protein that binds to the TFIIH core components XPD and p52 (7, 22, 60) and controls the steady-state level of cellular TFIIH in human fibroblasts (17, 51). TTDA appeared to be the sole TFIIH subunit dispensable for transcription *in vitro*; however, its presence stimulates this reaction (1), and the TTDA component is present in the preincision complex (PIC) and is required for transcription *in vivo* in yeast (35). TTDA exists in two cellular pools, a TFIIH-bound nuclear pool and a free pool that shuttles passively (due to its small size) from the cytoplasm to the nucleus (18). During active NER, TTDA binds more tightly to TFIIH and possibly plays a role in stabilizing TFIIH on lesions to allow the transition between NER intermediates (18). This NER-dependent TFIIH stabilization role can also partly restore the DNA repair deficiency in p52 *Drosophila melanogaster* mutants (Dmp52) when enough TTDA molecules are available (1). Moreover, it was found that TTDA is important for the DNA damage-dependent ATPase activity of XPB, stimulating the opening of the helix and the translocation of XPA to UV-damaged DNA (7). Coin and coworkers (7) further suggested that without TTDA, TFIIH, although loaded on the damaged DNA, cannot recruit the subsequent NER factors and that in its absence NER is fully compromised. Based on these observations, TTDA was suggested to be specifically required for the NER reaction. Indeed TTD-A primary fibroblasts exhibit a rather low level of UV-induced unscheduled DNA synthesis (UDS), the levels of which range from 10% (TTD13/14PV) to 25% (TTD1BR) of residual UDS activity (17), indicative of a severe NER defect. Surprisingly, however, the UV sensitivity of TTD-A primary fibroblasts is relatively mild compared to other complementation groups (e.g., XP-A, XP-B, and XP-G) with similarly low UDS levels (17). Because of this seeming discrepancy, we further studied the repair kinetics and the binding kinetics of TFIIH downstream NER factors to damaged sites in TTD-A cells. Our results show that TTD-A cells do not repair UV lesions at early time points after UV irradiation, explaining the low UDS levels. However, at later time points post-UV irradiation (6 to 8 h), most of the UV-induced 6-4PPs appeared to be removed. In addition, we found that the binding of downstream NER factors on damaged DNA is not completely abolished but retarded. Our results suggest that in TTD-A cells repair is not fully compromised but only retarded, which explains the relatively mild photosensitive phenotype observed in patients.

## MATERIALS AND METHODS

**Cell culture and specific treatments.** The primary human fibroblast strains used were XP12RO (XP-A), TTD1BR (TTD-A), TTD99RO (TTD-A), TTD14PV (TTD-A), and the NER-proficient C5RO cell line. The cells were cultured in Ham's F10 (Gibco) supplemented with antibiotics and 10% fetal calf serum at 37°C, 3% $O_2$, and 5% $CO_2$.

The simian virus 40 (SV40)-immortalized human cell lines used were XP2OS-sv (XP-A), TTD1BR-sv (TTD-A), and TTD1BR-sv (TTD-A), stably expressing TTDA-hemagglutinin (HA) and the NER-proficient MRC5-sv cell line. The cell lines were cultured in a 1:1 mixture of Ham's F10 and Dulbecco's modified Eagle's medium (DMEM) (Gibco) supplemented with antibiotics and 10% fetal calf serum at 37°C, 20% $O_2$, and 5% $CO_2$.

Treatment with UV-C (254 nm) was performed using a Philips germicidal lamp. Doses of 5 J/m$^2$ for enzyme-linked immunosorbent assay (ELISA) on primary fibroblasts; 25 J/m$^2$ for chromatin immunoprecipitation (ChIP); and 1, 2, 4, and 8 J/m$^2$ for UV survival were used for total irradiation. For local irradiation through a microporous filter (5 μm), a dose of 60 J/m$^2$ was used.

**UV cell survival.** Primary fibroblasts were plated on 6-well culture dishes ($5 \times 10^3$ per well) in quadruplicate (0 J/m$^2$) or triplicate (others) in 3 ml medium. Two days after seeding, the cells were washed with phosphate-buffered saline (PBS) and UV irradiated at various doses. The cells were pulse-labeled 5 days after irradiation with [*methyl*-$^3$H]thymidine (40 to 60 Ci/mmol; 5 μCi/ml), chased for 30 min in unlabeled medium, washed with PBS, lysed in 0.25 M NaOH, and harvested. The cell lysates were transferred into scintillation flasks and supplemented with 7.5 ml Hionic Fluor scintillation fluid (Packard). Each sample was counted in the scintillation counter for 10 min, and the results were expressed as the percentage of surviving cells at a given dose over the nonirradiated cells.

**UV-induced UDS.** Three days before the UDS assay (52), wild-type (WT) or XP-A primary fibroblasts were labeled with latex beads (0.79 μm) by adding a suspension of beads to normal culture medium (54). After trypsinization, the labeled primary fibroblasts were extensively washed to remove free beads. Cells ($0.5 \times 10^6$) were mixed in a 1:1 ratio with different TTD-A primary fibroblasts seeded on 24-mm coverslips, and after 2 days, they were irradiated with 16 J/m$^2$ UV-C. At various time points after UV irradiation, the cells were incubated for 2 h with culture medium containing 10 μCi [*methyl*-$^3$H]thymidine (110 Ci/mmol; Amersham Biosciences)/ml, washed with PBS, and fixed. Coverslips with radioactively labeled cells were mounted onto slides and dipped in a photosensitive emulsion (Ilford K2). After exposure (2 to 7 days), the slides were developed and stained. Repair capacity was quantified by counting autoradiographic grains above the nuclei of at least 25 cells. UDS levels are expressed as either an absolute grain count per nucleus (Fig. 1c) or the percentage of UDS in wild-type cells assayed directly after UV irradiation (0 to 2 h), which was set at 100% (Fig. 1b).

**Quantification of 6-4PP and CPD UV photoproducts by ELISA.** Seventy to 80% confluent cultures of cells to be analyzed were washed with PBS, UV irradiated, and incubated for various times. Cells were harvest in PBS, and DNA was isolated using a QIAamp DNA Blood Mini Kit (Qiagen). Concentrations were measured by the optical density at 260 nm. Ninety-six-well polyvinylchloride flat-bottom microtiter plates were precoated with 0.003% protamine sulfate (50 μl/well; Sigma) and dried in the dark overnight at 37°C. DNA samples were denatured for 10 min at 95°C and immediately cooled on ice for 20 min. Vortexed DNA solution (50 μl/well) was loaded in the precoated 96-well dish to a final concentration of 6 μg/ml for the detection of 6-4PP or 0.3 μg/ml for CPD. The plate was dried overnight at 37°C and washed 5 times with PBS plus 0.05% Tween 20 (150 μl/well). The wells were preabsorbed with PBS plus 2% fetal calf serum (FCS) for 30 min at 37°C and subsequently washed 5 times with PBS-Tween 20 prior to incubation with 100 μl/well primary antibody: 6-4PP (1:1,000; Bioconnect/MBL) or CPD (1:1,000; TDM-2; Bioconnect/MBL) diluted in PBS. After 5 washes with PBS-Tween 20, samples were incubated for 30 min at 37°C with a secondary antibody, goat anti-mouse IgG(H+L) conjugated to horseradish peroxidase (HRP) (1:2,000; Southern Biotech). After 5 washes with PBS-Tween 20, samples were treated with 100 μl/well citrate-phosphate buffer (24 mM $C_6H_8O_7 \cdot H_2O$ and 41 mM $Na_2HPO_4 \cdot 2H_2O$; Sigma). Samples were then incubated with 100 μl/well of freshly made ODP buffer (0.4% *o*-phenylene diamine and 0.02% citrate-phosphate buffer; Sigma) at 37°C for 30 min. The reaction was stopped by adding 50 μl/well of 2 M $H_2SO_4$, and absorbance was directly measured at 490 nm.

**Immunofluorescence.** Cells were grown on glass coverslips (24 mm) for 3 days prior to the experiments and fixed with 2% paraformaldehyde at 37°C for 15 min. Coverslips were washed with PBS containing 0.1% Triton X-100 three times for 5 min each time. To visualize the DNA photoproducts, nuclear DNA was denatured by incubation with 0.07 N NaOH at room temperature for 5 min, washed with 0.1% Triton X-100 three times for 5 min each time, and subsequently washed with PBS$^+$ (PBS containing 0.15% glycine and 0.5% bovine serum albumin [BSA]). The cells were incubated at room temperature with primary antibodies for 2 h in a moist chamber. Subsequently, the coverslips were washed three times with PBS–Triton X-100 and PBS$^+$, incubated for 1 h with secondary

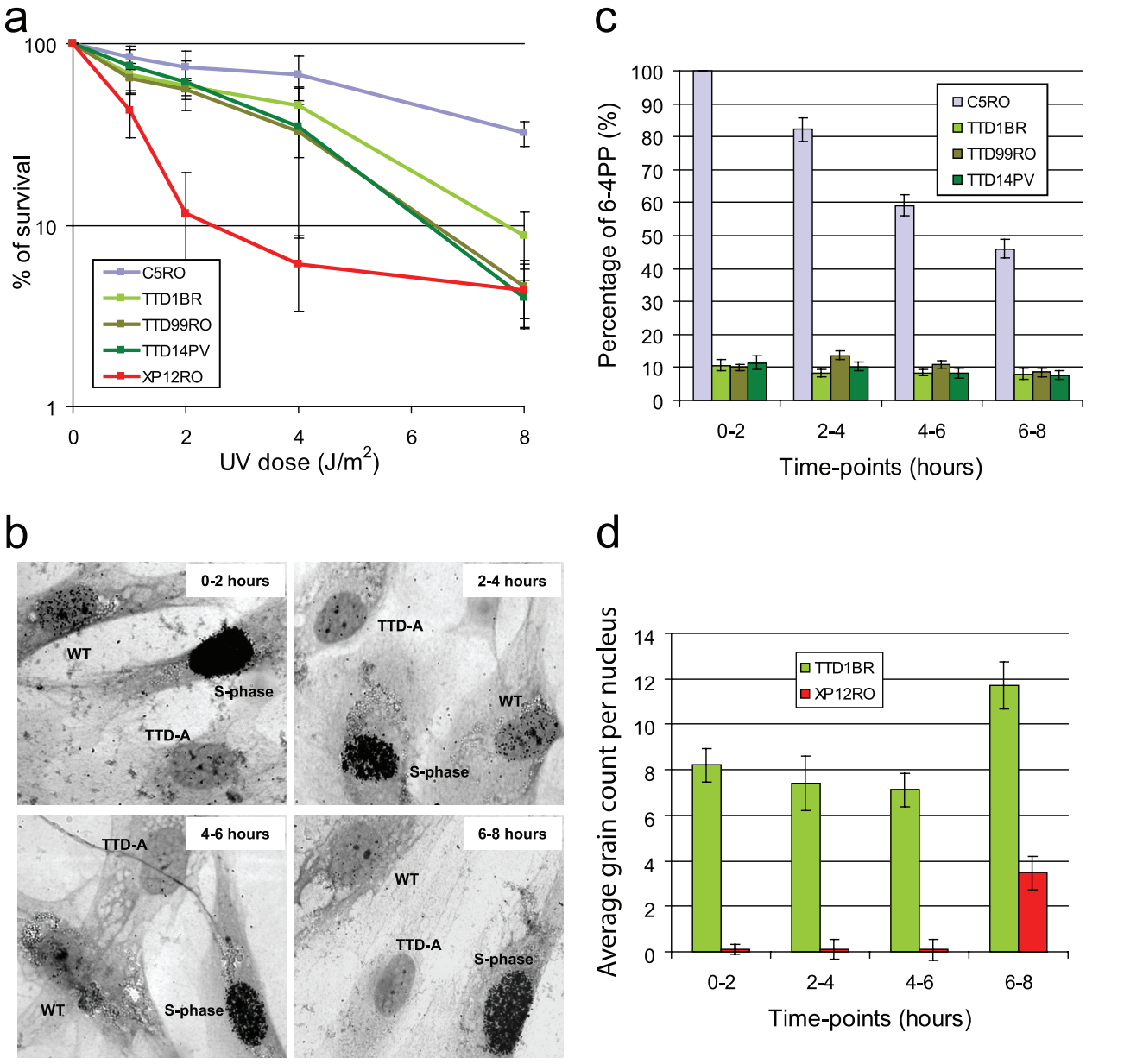


FIG. 1. Time-lapse UDS capacity. (a) Graph showing the surviving fraction of cells after different doses of UV irradiation of wild-type C5RO, TTD-A, and XP-A primary fibroblasts. The percentage of surviving cells was plotted against the applied UV dose, measured by [$^3$H]thymidine incorporation. The error bars indicate the standard errors of the mean (SEM). (b) Representative pictures of UDS experiments of TTD-A (TTD1BR) mixed with WT (C5RO) primary fibroblasts at different time points, as indicated, after UV irradiation. WT cells are recognized by the presence of small beads in the cytoplasm, and the heavily labeled cells are in S phase. (c) Graph showing the relative UDS levels at different time points after UV irradiation obtained after counting the autoradiographic grains above the nuclei expressed as percentages of wild-type UDS measured directly after UV irradiation, which was set at 100%. The UDS levels of the different TTD-A primary fibroblasts are indicated in green. The error bars indicate the SEM of at least 25 nuclei counted. (d) Graph showing the absolute UDS levels at different time points after UV irradiation obtained after counting the autoradiographic grains above the nuclei of TTD-A (TTD1BR) and XP-A (XP12RO) primary fibroblasts. The error bars indicate the SEM of at least 50 nuclei counted.

antibodies at room temperature, and again washed three times in PBS–Triton X-100. Samples were embedded in Vectashield mounting medium (Vector Laboratories, Burlingame, CA). Images were obtained by confocal laser scanning microscopy imaging, carried out with an LSM 510 microscope (Zeiss, Oberkochen, Germany).

For this procedure, the primary antibodies used were rabbit anti-XPA (1:2,000; kindly provided by K. Tanaka), rabbit anti-XPB (1:1,000; S-19; Santa Cruz Biotechnology), rabbit anti-XPC (1:1,000) (48), mouse anti-CPD (1:1,000; TDM-2; BioConnect/MBL), and rat anti-HA (1:500; 3F10; Roche). The secondary antibodies used were Cy3-conjugated goat anti-mouse antiserum (1:1,000; Jackson ImmunoResearch Laboratories), Alexa Red-conjugated goat anti-rabbit antiserum (1:1,000; Molecular Probes), Alexa Fluor 350 goat anti-mouse antiserum (1:250; Molecular Probes), and Alexa Green 488 goat anti-rat antiserum (1:1,000; Molecular Probes).

**Cross-linking and ChIP.** *In vivo* cross-linking to identify chromatin-bound NER proteins 1 h after UV irradiation (ChIP on Western) was performed as previously described (15): 20 confluently grown petri dishes (14.5 cm) for each sample were treated with freshly prepared 1% formaldehyde solution containing

50 mM HEPES, pH 8.0, 1 mM EDTA, 0.5 mM EGTA, and 0.1 M NaCl for 16 min at 4°C. Cross-linking was stopped by adding glycine to a final concentration of 0.125 M. The cells were washed with cold PBS and isolated after centrifugation (1,300 rpm for 5 min). Cell lysis was achieved by rotation of the cell pellet resuspended in 7 ml of PDB buffer (50 mM HEPES, pH 7.8, 1 mM EDTA, 0.5 mM EGTA, 0.15 M NaCl, 0.5% NP-40, 0.25% Triton X-100, 10% glycerol, 1 mM phenylmethylsulfonyl fluoride [PMSF], and 5 μg/ml proteinase inhibitors) at 4°C for 10 min. The resulting nuclei were collected by centrifugation (1,300 rpm for 5 min) and washed with 7 ml buffer (10 mM Tris-HCl, pH 8.0, 1 mM EDTA, 0.5 mM EGTA, 0.2 M NaCl, 1 mM PMSF, and 5 μg/ml proteinase inhibitors). The crude nuclei were resuspended in 2.5 ml of 1× RIPA buffer (PBS containing 1% NP-40, 0.5% Na deoxycholate, and 0.1% SDS) and sonicated (power setting 5) on ice using repeated 20-s bursts with a Soniprep 150 (Beun De Ronde), followed by 1 min of cooling on ice between sonications to obtain DNA fragments with an average length of 0.3 to 0.7 kb. Samples were centrifuged at 13,000 rpm for 45 min at 4°C, and the supernatants were stored at −80°C. The DNA size was regularly checked between sonication steps by electrophoresis on agarose after proteinase K treatment and phenol chloroform extraction.

Cross-linked cellular extracts were incubated overnight at 4°C in RIPA buffer with rabbit polyclonal anti-XPB (S-19; Santa Cruz Biotechnology) or normal rabbit IgG (Santa Cruz Biotechnology) cross-linked to protein A-Sepharose beads (Amersham Biosciences). Before immunoprecipitation, the cross-linked beads were preabsorbed with 100 μg/ml sonicated (denatured) salmon sperm DNA and 100 μg/ml BSA for 2 h at 4°C. After immunoprecipitation, the beads were washed twice with 1× RIPA buffer, once with RIPA buffer containing 100 μg/ml single-stranded DNA (ssDNA), and twice with 1× RIPA buffer containing 100 μg/ml ssDNA plus 0.5 M NaCl. Finally, the beads were washed with LiCl buffer (20 mM Tris, pH 8.0, 1 mM EDTA, 250 mM LiCl, 1% Na deoxycholate, 1 mM PMSF, and 5 μg/ml proteinase inhibitors). For protein analysis, beads were mixed with an equal volume of 2× SDS-sample buffer and boiled for 30 min to 1 h at 94°C. Proteins were separated on 8% SDS-PAGE and transferred to 0.45-μm nitrocellulose membranes (Millipore). The membranes were hybridized with either rabbit polyclonal ERCC1 (1:1,000) (50), rabbit polyclonal XPF (1:1,000; affinity purified), mouse monoclonal anti-p62 (3C9), or rabbit anti-XPA (1:1,000; kindly provided by K. Tanaka) antibody, followed by a secondary antibody (either donkey anti-rabbit or rabbit anti-mouse) conjugated with horseradish peroxidase (Biosource International) and detected using enhanced chemiluminescence (ECL+ Detection Kit; Amersham Biosciences).

## RESULTS

**Prolonged residual UDS levels in TTD-A primary fibroblasts.** To gain further insight into the apparent discrepancy between low UDS and relatively mild UV sensitivity of TTD-A cells, we systematically analyzed the NER parameters of the three different TTD-A primary fibroblasts (TTD1BR, TTD99RO, and TTD14PV) in a time-resolved manner. First, we systematically determined the UV hypersensitivities of the different TTD-A primary fibroblasts assayed in parallel in the same experiment. As shown in Fig. 1a, all TTD-A primary fibroblasts exhibit markedly similar and mild UV sensitivities compared to a completely NER-deficient (XP-A) primary fibroblasts. Next, we determined the UDS levels of these three TTD-A patient cells and of NER-proficient wild-type primary fibroblasts (C5RO) at different time points after UV irradiation. To avoid systematic intersample variations of UDS measurements, we performed these measurements in a setup in which, for each of the separate cell strains used and time points measured, the same internal wild-type control was included. To that end, we labeled wild-type primary fibroblasts (C5RO) with latex beads and mixed them with unlabeled TTD-A primary fibroblasts (Fig. 1b). Residual UDS levels were quantified and expressed as percentages of the UDS of wild-type cells assayed simultaneously (Fig. 1c). The repair capacity of all the known TTD-A primary fibroblasts was around 10% of wild-type levels when measured directly after UV irradiation (labeled with [$^3$H]thymidine between 0 and 2 h post-UV irradiation). This low level of UDS in TTD-A primary fibroblasts remained constant over a long period (6 to 8 h) post-UV irradiation, whereas wild-type primary fibroblasts showed a gradual reduction over time of UDS levels (Fig. 1c). Under the same conditions, we labeled XP-A primary fibroblasts with latex beads, mixed them with unlabeled TTD-A primary fibroblasts, and measured UDS levels at the various time points (Fig. 1d). The absolute grain count measured in TTD-A cells was significantly higher than in XP-A primary fibroblasts (indistinguishable from non-UV-induced UDS), showing that this persistent low level of UDS is not background staining. Our results suggest that the incorporation of nucleotides during NER-induced DNA synthesis at the site of damage (i.e., the penultimate gap-filling step of the NER process) is not completely abolished but slowly progresses in TTD-A primary fibroblasts.

**Retarded 6-4PP removal in TTD-A cells.** The low but persistent UDS can be explained by slow but continuous UV-induced lesion removal in TTD-A cells. UDS in the first hours after UV irradiation in NER-proficient cells is mainly derived from 6-4PP repair (29, 37), and the majority of these lesions are removed within 4 to 6 h after UV irradiation (49). To verify whether the observed low, continuous UDS is in part derived from partial and slow repair of 6-4PP, we determined 6-4PP elimination kinetics in primary fibroblasts by using ELISA (31) (Fig. 2a). At different time points after UV irradiation (5 J/m$^2$), DNA was isolated, and the number of UV-induced lesions was determined in wild-type (blue), TTD-A (green hues), and XP-A (red) (the last are fully NER deficient) primary fibroblasts. As previously determined (11, 49), we also found that in wild-type cells the vast majority of 6-4PP lesions were removed within only 2 h after UV irradiation (Fig. 2a). In accordance with the low but persistent UDS, TTD-A primary fibroblasts do exhibit 6-4PP lesion removal (Fig. 2a). This removal, however, is severely delayed compared to wild-type cells, with approximately 5 to 20% removal of 6-4PPs in 2 h and 50 to 75% repair after 8 h. In contrast, NER-deficient primary fibroblasts from an XP-A patient (XP12RO) were fully deficient in repairing 6-4PP even after 8 h. Under the same experimental conditions, the CPD removal was also measured in these primary fibroblasts (Fig. 2b). Due to their structural properties, CPD lesions are poor substrates for NER, and its removal is less efficient. As expected, NER-deficient primary fibroblasts were unable to repair CPD lesions even after 24 h. NER-proficient primary fibroblasts completely remove CPD lesions within 16 h after UV irradiation. Surprisingly, CPD removal as measured in two independent TTD-A primary fibroblasts (TTD1BR and TTD99RO) showed virtually the same CPD repair kinetics as measured in a NER-proficient cell line. These experiments clearly show that the slow repair kinetics measured in TTD-A primary fibroblasts is solely dependent on inefficient 6-4PP removal.

**Delayed NER complex assembly in TTD-A cells.** Previously, the TTD-A NER defect was explained by the observed absence of NER complex assembly in experiments using local UV damage induction (7). In these experiments, however, assembly of NER factors was determined at only a single time point (i.e., 30 min) after UV irradiation. As we found retarded damage removal in TTD-A cells here, slower NER factor assembly at damaged DNA can also be envisaged. To determine whether the delayed repair observed in TTD-A cells is derived from inefficient NER complex assembly, we investigated the accu-

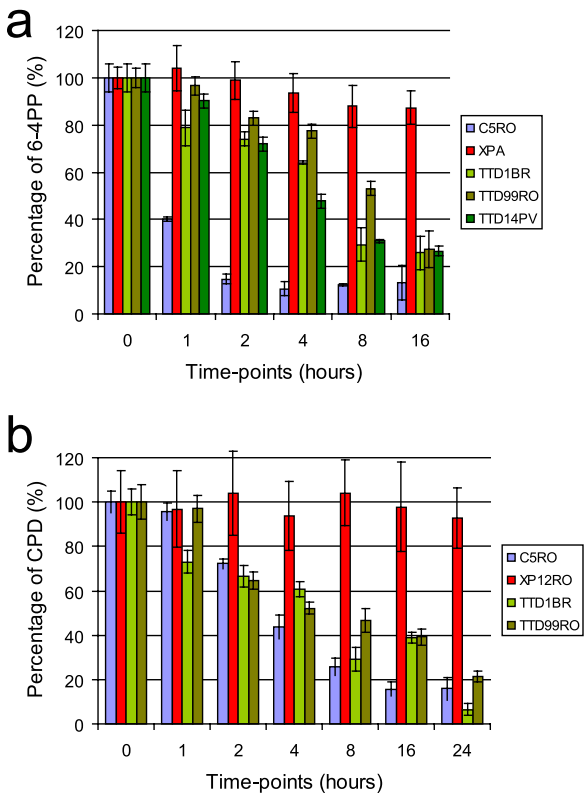


FIG. 2. UV photolesion repair. Wild-type (C5RO), TTD-A (TTD1BR, TTD99RO, and TTD14PV), and XPA (XP12RO) primary fibroblasts were grown in a 14.5-cm dish. The cells were washed with PBS and UV irradiated at 5 J/m$^2$. DNA was isolated at different time points (0, 1, 2, 4, 8, 16, and 24 h) after UV irradiation. (a) Amount of 6-4PP measured by ELISA, using a 6-4PP-specific antibody. The amount of 6-4PP measured directly after UV irradiation was set at 100%. (b) Amount of CPD measured by ELISA, using a CPD-specific antibody. The amount of CPD measured directly after UV was set at 100%.

mulation of several NER proteins at local UV-damaged (LUD) sites over time, using comparative immunofluorescence (51). A mixed cell population containing both TTD-A and TTD-A corrected cells that stably express TTDA-HA (18) (here, wild-type cells) was subjected to local-damage irradiation. LUD was visualized using a CPD antibody, and to distinguish TTDA-HA corrected cells from TTD-A cells, an HA antibody was used. Initially, we tested XPC binding (Fig. 3a and Table 1) on LUDs, as XPC is one of the first proteins that recognized the UV-damaged DNA, and its binding to lesions is responsible for the subsequent recruitment of TFIIH to the emerging chromatin-bound NER complex. As expected, XPC was able to rapidly accumulate at the sites of lesions in both wild-type and TTD-A cells, since the accumulation of XPC is independent of TFIIH status (45, 57, 59). However, 4 h after UV irradiation, when the 6-4PP lesions are mostly repaired in wild-type cells and XPC is undetectable at LUD in these cells, XPC remains clearly visible at LUD in TTD-A cells, showing that UV lesions are still not fully repaired in these cells. We next tested the binding of TFIIH to NER complexes by visualizing the XPB helicase subunit at the LUD with an XPB-specific antibody (Fig. 3b). While in wild-type cells XPB accumulates very rapidly at LUD, TFIIH recruitment in TTD-A cells is severely delayed but persists at these sites at least up to 4 h after UV irradiation (Fig. 3b and Table 1). After TFIIH binding to damaged DNA, XPA is recruited to the growing NER complex (57), and this recruitment was found to be completely abolished in TTD-A cells (7). However, we found that XPA accumulated at LUD with the same slower kinetics in TTD-A cells as TFIIH (Fig. 3c, Table 1), showing that as soon as sufficient TFIIH is loaded, XPA also becomes visible at LUD. It is surprising to note that XPA remains visible even 4 h post-UV irradiation in wild-type (TTDA-HA corrected) cells, in contrast to the other tested preincision NER factors, XPC and TFIIH. Although this sustained XPA binding at LUD was previously also observed in live-cell microscopy using green fluorescent protein (GFP)-tagged XPA (27), thereby excluding an artifact introduced by the immunofluorescence procedure, we currently do not have a satisfactory mechanistic explanation for this prolonged XPA binding to LUD other than that XPA has an additional unknown function(s) in NER beyond damage verification. Next to XPA, other downstream NER factors (whose incorporation into NER complexes was also dependent on functional TFIIH), such as ERCC1 and XPF, also slowly accumulate at LUD (data not shown).

**Inefficient chromatin-bound NER complex formation in TTD-A cells.** The delayed or inefficient NER complex assembly in TTD-A cells could in theory also be derived from the reduced TFIIH steady-state level observed in TTD-A cell lines (51). To investigate whether the reduced NER complex formation is derived from an improperly structured TFIIH complex or could be attributed to a reduced amount of TFIIH, we directly analyzed the interactions between TFIIH and the other NER factors within chromatin-bound NER complexes by performing a variant of ChIP (15). In this assay, immunoprecipitation and sample preparation were performed as in classical ChIP, though rather than analyzing the coprecipitating genomic DNA, we analyzed the chromatin-bound interacting proteins (ChIP on Western) that coprecipitated with an XPB antibody (TFIIH subunit) (see Materials and Methods). As expected, chromatin-bound association between TFIIH and the ERCC1-XPF complex was dependent on UV irradiation (Fig. 4a). Next, we analyzed the chromatin-bound and UV-induced TFIIH-interacting proteins in wild-type (MRC5-SV) and TTD-A cells and compared them to completely NER-deficient cells (XP-A). To exclude the possibility that the inefficient recruitment of XPA and ERCC1-XPF to the NER complex could be a consequence of the low TFIIH steady state, we normalized TFIIH quantities (on the basis of anti-p62 staining, another core component of TFIIH) by loading equal amounts of precipitated TFIIH (Fig. 4b). We were able to visualize a significant UV-induced increase in the loading of XPA and ERCC1-XPF to the chromatin in NER-proficient cells. As expected, XPA and ERCC1-XPF binding to chromatin was abolished in XP-A cells. Importantly, clearly less efficient XPA and ERCC1-XPF were also coprecipitated in TTD-A cells compared to wild-type cells. These data suggest that it is not the amount of TFIIH but the physical and chemical constitution of TFIIH in the absence of TTDA that does not allow proper loading of downstream NER factors.

In addition, this ChIP on Western analysis provided independent evidence that in TTD-A cells NER complex formation

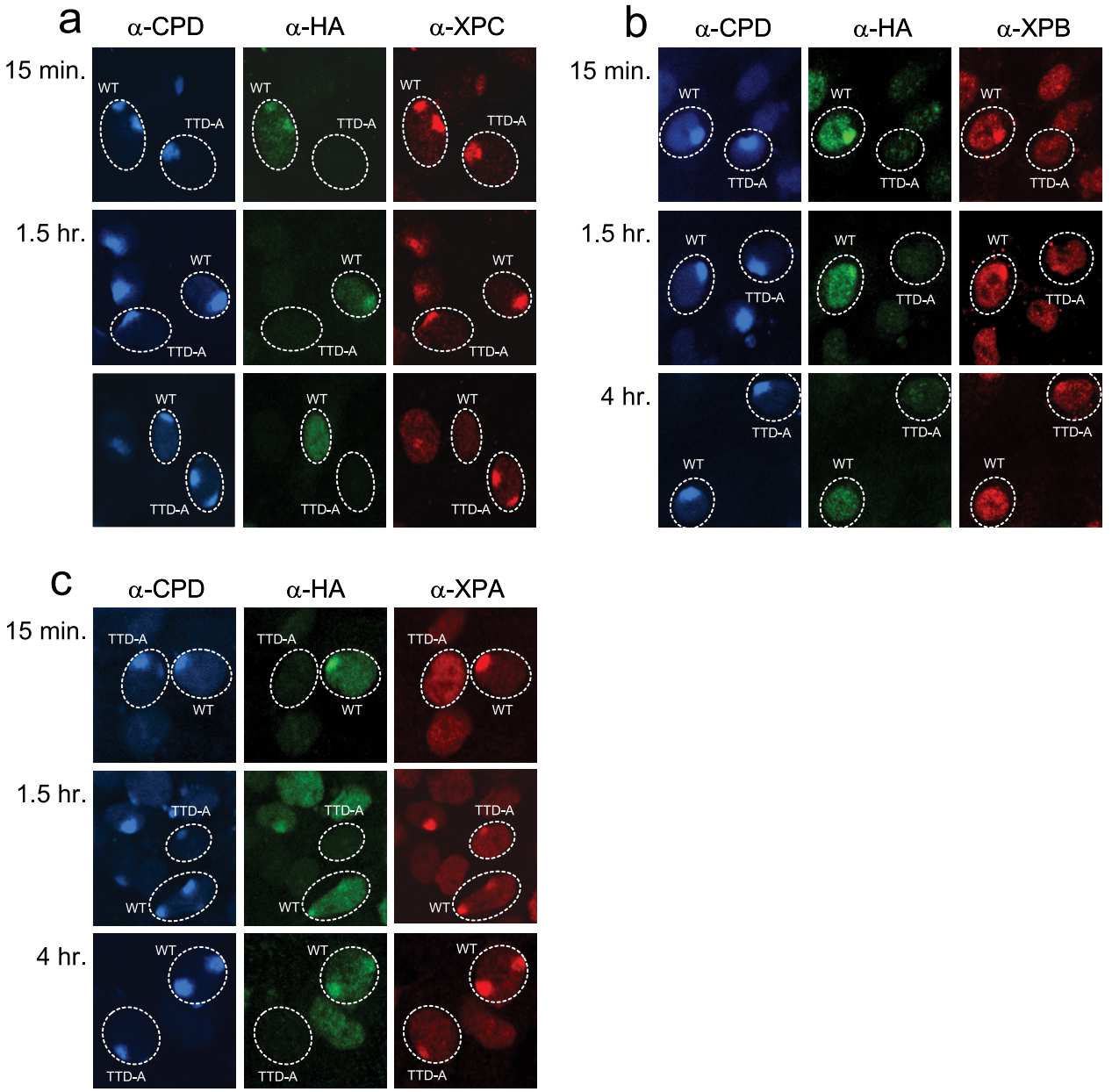


FIG. 3. Recruitment of NER proteins to sites of local UV damage. Triple-color immunofluorescence analysis of NER factor recruitment to LUD spots in TTD-A and TTD-A corrected (TTDA-HA) cells. Three days prior to analysis, cells were seeded in a 1:1 ratio on coverslips. The cells were irradiated at 60 J/m$^2$ through a filter containing 5-μm pores. The cells were fixed at different time points after UV irradiation (15 min and 1.5 and 4 h), and immunofluorescent staining was performed using antibodies against CPDs (blue) (marker for LUD), HA (green) (to discriminate between TTD-A and corrected TTD-A cells), and XPC (a), XPB (b), or XPA (c) (red).

TABLE 1. Recruitment of NER proteins to chromatin after UV irradiation

| Protein | Recruitment[a] | | | | | |
|---|---|---|---|---|---|---|
| | WT | | | TTD-A | | |
| | 15 min | 1.5 h | 4 h | 15 min | 1.5 h | 4 h |
| XPC | + | + | − | + | + | + |
| XPB | + | + | − | − | + | + |
| XPA | + | + | + | − | + | + |

[a] At the indicated time points, the recruitment of different NER proteins to LUD sites was scored. Accumulations are scored with a minus for no accumulation or a plus for accumulation.

can occur, though only in a very inefficient manner, and thus confirmed the conclusion obtained from the immunofluorescence studies.

## DISCUSSION

Mutations in the TFIIH subunits XPB, XPD, and TTDA are associated with a surprising clinical variation ranging from cancer-prone XP to the severe neurodevelopmental and premature-ageing syndromes TTD, cranio-oculo-facial syndrome (COFS), and XP combined with CS or TTD (3, 5, 16, 19, 25, 41, 42, 53).

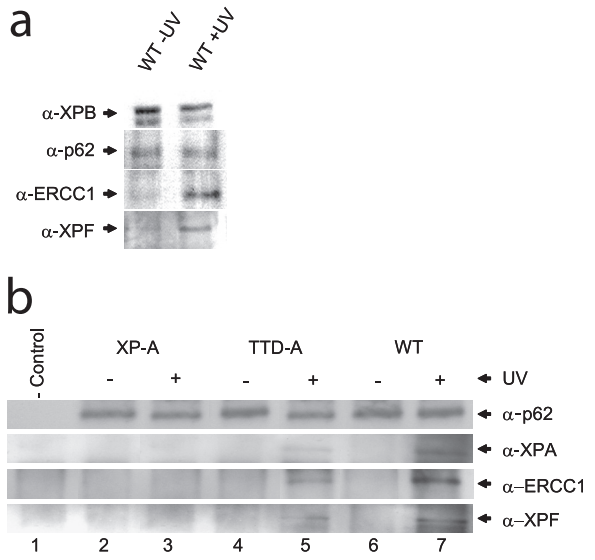


FIG. 4. Recruitment of NER proteins to chromatin after UV irradiation. (a) Western on ChIP was performed on extracts isolated after formaldehyde cross-linking of wild-type (MRC5-SV) cells (with and without 25 J/m$^2$ UV irradiation; 1 h after irradiation) using an XPB-specific rabbit polyclonal antibody. Equal amounts of precipitated TFIIH were loaded (analyzed by anti-XPB and anti-p62 immunostaining [top two rows]). Under these conditions, a strong increase in the NER endonuclease complex ERCC1-XPF (bottom two rows) was observed to coprecipitate with chromatin-bound TFIIH after UV irradiation. (b) Western on ChIP analysis of XP-A (XP2OS-SV, lanes 2 and 3), TTD-A (TTD1BR-SV, lanes 4 and 5), and wild-type (MRC5-SV, lanes 6 and 7) cells from UV-treated (+) or mock-treated (−) cells, as in panel a. Equal amounts of precipitated TFIIH (anti-p62 signal) were loaded. The immunoprecipitated material was probed for XPA, ERCC1, and XPF and compared to nonspecific precipitated material (lane 1) from preimmune rabbit IgG. In XP-A cells, XPA, ERCC1, and XPF do not coprecipitate after UV irradiation, whereas in TTD-A cells, strongly reduced amounts of these proteins were coprecipitated with TFIIH after UV irradiation.

Thus far, only patients expressing the TTD phenotype have been found to be associated with inherited mutations in the *TTDA* gene (17, 40). Among TTD patients, the spectrum of clinical features is very broad and stretches from very mild forms of the disease (with normal development and only the brittle-hair phenotype) to very severe cases (characterized by high mortality at a young age and severe developmental defects) (12). TTD-A patients present in general a relatively mild form of TTD, including moderate UV hypersensitivity (17, 42, 47). It is remarkable to note that the repair properties of TTD-A primary fibroblasts present a puzzling picture, as the mild UV sensitivity is accompanied by very low UV-induced UDS (17, 51). In other NER-deficient XP cells, such as XP-D, XP-A, or XP-G, that present similar low levels of UDS, UV sensitivity appeared much more pronounced. This apparent discrepancy has drawn our attention to thoroughly analyzing the repair properties of TTD-A cells. NER-induced DNA synthesis measurements are generally conducted within the first 2 h after UV irradiation, whereas UV survival measurements extend over a few days after the initial damaging event. Based on these two entirely different time scales of monitoring DNA repair endpoints, we hypothesize that the repair activity in TTD-A cells is not completely deficient but progresses slowly. When repair continues at a slower pace, the UV-induced lesions that are mainly responsible for cytotoxicity (6-4PP) could be gradually removed during the extended time between irradiation and colony survival measurement. Indeed, in our time-resolved UDS experiments, we showed that the low level of UDS in TTD-A cells progresses at more or less the same rate to at least 8 h after UV irradiation. Within this time frame, the UDS gradually declines in NER-proficient cells assayed in parallel. In addition, the actual 6-4PP removal is not completely absent in TTD-A cells, though it is severely retarded (Fig. 2a). The continuous slow removal of 6-4PP still repairs most of these lesions within a reasonable time (75% within 6 h, whereas 85% is removed within 3 h in WT cells [Fig. 2a]), thus explaining the only moderate UV sensitivity, in line with our hypothesis. Surprisingly, CPD removal was not retarded in TTD-A primary fibroblasts but showed repair kinetics similar to those of a NER-proficient cell line (Fig. 2b). This observation supports the hypothesis that 6-4PP lesions are the main lesions that are repaired with slower repair kinetics in TTD-A primary fibroblasts. Apparently, for the repair of CPD lesions, other NER-associated factors are more important for determining the rate of NER complex formation and actual removal of CPD lesions. This observation is remarkably different from the repair parameters measured in other non-*TTDA* mutated TTD (XP-B or XP-D) cells. In fact, it has been shown that, in XP-D mutated TTD primary fibroblasts, the 6-4PP repair capacity is highly variable and depends on the mutation in the *XPD* gene: 6-4PPs are either repaired normally, as in TTD1VI cells (R722W), or not repaired at all in TTD9VI (R112H) cells (6). In addition, in XP-B/TTD primary fibroblasts, TTD6VI (amino acid [aa] 355 mutated [58]) 6-4PPs are efficiently repaired (36). Although 6-4PP removal appeared highly variable throughout the different NER-deficient TTD cells, delayed repair, as in TTD-A cells, was never observed. In conclusion, the retarded repair of 6-4PP observed in TTD-A cells appeared to be a specific feature of this complementation group.

Previously, it was found that the absence of TTDA inhibits the ATPase activity of XPB, thereby hindering the opening of the DNA, and it was suggested that this defect precludes the subsequent loading of XPA (7). In contrast to these observations, we were able to show that, in TTD-A cells, XPA can still be loaded on damaged DNA, although with much lower efficiency and slower kinetics than in wild-type cells. As a matter of fact, XPA binding to LUD followed almost the same kinetics as TFIIH, suggesting a scenario in which XPA is recruited once sufficient mutated TFIIH is properly loaded on the damaged sites. The discrepancy between the present study and the work of Coin and collaborators (7) can be explained by different detection thresholds of the antibodies used in the two studies and the single time point (30 min post-UV irradiation) analyzed in the Coin study. Based on our data, we favor a different scenario, in which the recruitment of the downstream NER factors of XPC is affected in TTD-A cells (Fig. 5) rather than only XPA. Importantly, the absence of TTDA seems to influence the assembly kinetics of TFIIH, XPA, and ERCC1-XPF (Fig. 3). This finding was further corroborated by ChIP experiments, showing that the binding capacity of XPA and ERCC1-XPF on damaged DNA in TTD-A cells is strongly reduced. We propose a model (Fig. 5) in which the absence of TTDA causes improperly folded/structured TFIIH that affects

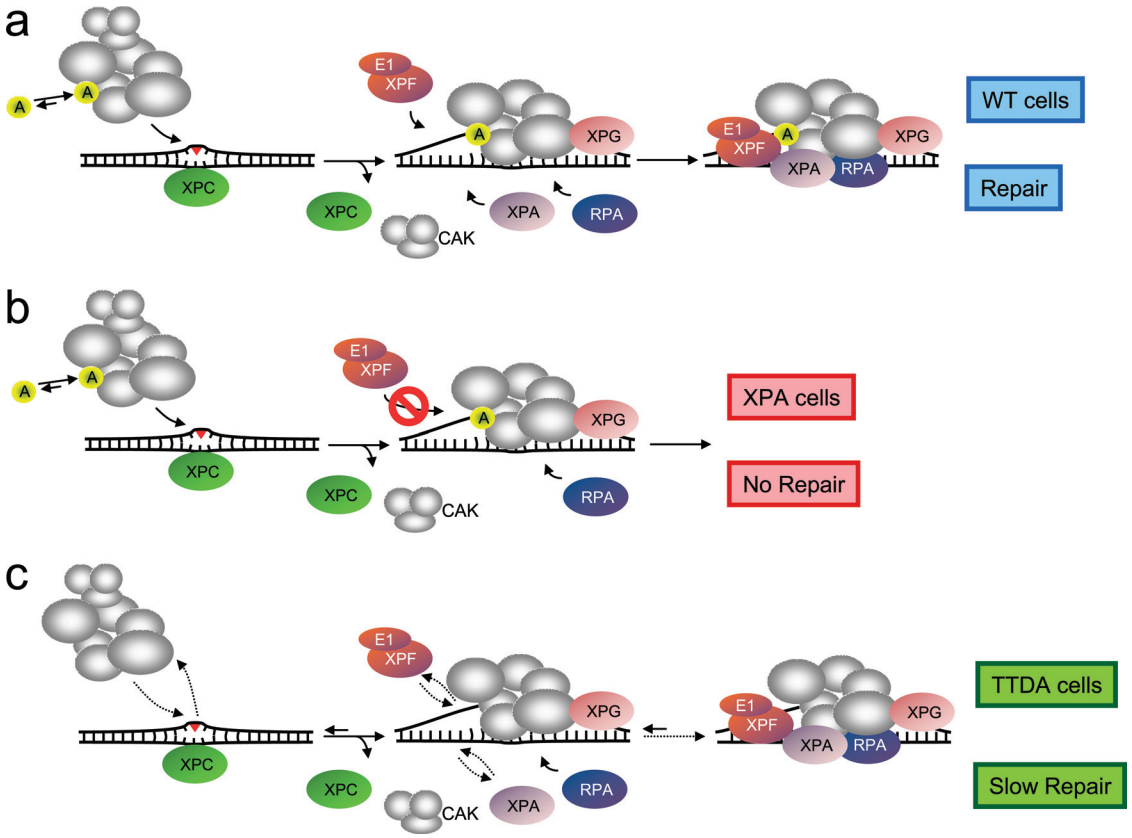


FIG. 5. Model for TTDA function in NER and proposed model for lesion-bound NER complex formation in wild-type, XP-A, and TTD-A cells. (a) In wild-type cells, XPC binds to UV lesions and recruits TFIIH and XPG, followed by XPA binding via its interaction with TFIIH. Under these conditions, TTDA (p8) is more stably bound to TFIIH and promotes the subsequent steps in NER complex formation and possibly stimulates the helicase activity of TFIIH. The unwound DNA structure is stabilized by the presence of TFIIH, XPA, and RPA; together, these proteins are required for recruiting the ERCC1-XPF complex via XPA interaction. After assembling the complete NER machinery, dual incision can occur, and these intermediates are further processed by gap-filling synthesis and ligation. (b) In XP-A cells, recruitment of XPC, TFIIH, and XPG occurs normally, including stable association of TTD-A. Nevertheless, due to the absence of XPA, downstream NER factors were not assembled, and thus NER activity is completely abolished. (c) In TTD-A cells, TFIIH stability and probably protein conformation have been altered because of the complete absence or the presence of a truncated TTDA protein. Efficient binding of mutated TFIIH is affected and reduces its affinity for the NER complex. Retarded binding of mutated TFIIH attracts XPA to the site of damage to stabilize the NER complex. Furthermore, incorporation of ERCC1-XPF into the NER complex is also retarded similarly to XPA. Nevertheless, although retarded, the assembly of the different NER factors takes place, and finally, DNA lesions are repaired.

not only the stability of TFIIH (51), but also efficient recruitment of subsequent NER factors. Nevertheless, although retarded, the assembly of the different NER factors still occurs, though with strongly decreased efficiency, and finally, DNA lesions are removed. From our previous studies, we know that the transient binding of TTDA to TFIIH is stabilized during active NER (18). We do not know, however, how this binding influences TFIIH structure when bound to lesions. It is possible that the observed interaction between TTDA, p52 (TFIIH core subunit), and XPD (22, 56) both modifies the XPB ATPase activity (7) of TFIIH and favors the affinity of downstream NER factors for the lesion-bound complex. Together, these actions create a more NER-efficient TFIIH complex that allows the incision step to occur (this paper). Previously, it was shown that overexpression of TTDA can partly rescue the UV sensitivity and NER defect in *D. melanogaster* p52 mutants (Dmp52) (1) and also suggested that the presence of TTDA renders TFIIH a NER-competent complex. In summary, our study sheds new light on the peculiar repair parameters of TTD-A cells and provides an explanation for the mild UV sensitivity in combination with a low UDS.

## ACKNOWLEDGMENTS

We thank K. Tanaka for kindly providing XPA antibody, M. Fousteri for help with the ChIP experiments, J. H. J. Hoeijmakers for helpful discussions, and A. Raams for technical assistance.

This study was financed by the Dutch Organization for Scientific Research (grants ZonMW 917-46-364 and 912-08-031; EU-FP6, IP DNA repair, and LSHG-CT-2005-512113; EU-FP6; and MRTN-CT-2003-503618 to W.V.), the Centre National de la Recherche Scientifique (CNRS contract no. 039438 to G.G.-M.), and the Institut National du Cancer (InCa contract no. 2009-001 to G.G.-M.).

## REFERENCES

1. **Aguilar-Fuentes, J., et al.** 2008. p8/TTDA overexpression enhances UV-irradiation resistance and suppresses TFIIH mutations in a Drosophila trichothiodystrophy model. PLoS Genet. **4**:e1000253.
2. **Bergmann, E., and J. M. Egly.** 2001. Trichothiodystrophy, a transcription syndrome. Trends Genet. **17:**279–286.
3. **Broughton, B. C., et al.** 2001. Two individuals with features of both xeroderma pigmentosum and trichothiodystrophy highlight the complexity of the clinical outcomes of mutations in the XPD gene. Hum. Mol. Genet. **10:**2539–2547.

4. **Broughton, B. C., H. Steingrimsdottir, C. A. Weber, and A. R. Lehmann.** 1994. Mutations in the xeroderma pigmentosum group D DNA repair/transcription gene in patients with trichothiodystrophy. Nat. Genet. **7:**189–194.
5. **Broughton, B. C., et al.** 1995. Molecular and cellular analysis of the DNA repair defect in a patient in xeroderma pigmentosum complementation group D who has the clinical features of xeroderma pigmentosum and Cockayne syndrome. Am. J. Hum. Genet. **56:**167–174.
6. **Chiganças, V., K. M. Lima-Bessa, A. Stary, C. F. Menck, and A. Sarasin.** 2008. Defective transcription/repair factor IIH recruitment to specific UV lesions in trichothiodystrophy syndrome. Cancer Res. **68:**6074–6083.
7. **Coin, F., et al.** 2006. p8/TTD-A as a repair-specific TFIIH subunit. Mol. Cell **21:**215–226.
8. **Conaway, R. C., and J. W. Conaway.** 1993. General initiation factors for RNA polymerase II. Annu. Rev. Biochem. **62:**161–190.
9. **Egly, J. M.** 2001. The 14th Datta lecture. TFIIH: from transcription to clinic. FEBS Lett. **498:**124–128.
10. **Evans, E., J. G. Moggs, J. R. Hwang, J. M. Egly, and R. D. Wood.** 1997. Mechanism of open complex and dual incision formation by human nucleotide excision repair factors. EMBO J. **16:**6559–6573.
11. **Eveno, E., et al.** 1995. Different removal of UV photoproducts in genetically related xeroderma pigmentosum and trichothiodystrophy diseases. Cancer Res. **55:**4325–4332.
12. **Faghri, S., D. Tamura, K. H. Kraemer, and J. J. Digiovanna.** 2008. Trichothiodystrophy: a systematic review of 112 published cases characterises a wide spectrum of clinical manifestations. J. Med. Genet. **45:**609–621.
13. **Fisher, R. P., and D. O. Morgan.** 1994. A novel cyclin associates with MO15/CDK7 to form the CDK-activating kinase. Cell **78:**713–724.
14. **Fousteri, M., and L. H. Mullenders.** 2008. Transcription-coupled nucleotide excision repair in mammalian cells: molecular mechanisms and biological effects. Cell Res. **18:**73–84.
15. **Fousteri, M., W. Vermeulen, A. A. van Zeeland, and L. H. Mullenders.** 2006. Cockayne syndrome A and B proteins differentially regulate recruitment of chromatin remodeling and repair factors to stalled RNA polymerase II in vivo. Mol. Cell **23:**471–482.
16. **Fujimoto, M., et al.** 2005. Two new XPD patients compound heterozygous for the same mutation demonstrate diverse clinical features. J. Investig. Dermatol. **125:**86–92.
17. **Giglia-Mari, G., et al.** 2004. A new, tenth subunit of TFIIH is responsible for the DNA repair syndrome trichothiodystrophy group A. Nat. Genet. **36:**714–719.
18. **Giglia-Mari, G., et al.** 2006. Dynamic interaction of TTDA with TFIIH is stabilized by nucleotide excision repair in living cells. PLoS Biol. **4:**e156.
19. **Graham, J. M., Jr., et al.** 2001. Cerebro-oculo-facio-skeletal syndrome with a nucleotide excision-repair defect and a mutated XPD gene, with prenatal diagnosis in a triplet pregnancy. Am. J. Hum. Genet. **69:**291–300.
20. **Guzder, S. N., et al.** 1994. DNA repair gene RAD3 of S. cerevisiae is essential for transcription by RNA polymerase II. Nature **367:**91–94.
21. **Hanawalt, P. C.** 2002. Subpathways of nucleotide excision repair and their regulation. Oncogene **21:**8949–8956.
22. **Kainov, D. E., M. Vitorino, J. Cavarelli, A. Poterszman, and J. M. Egly.** 2008. Structural basis for group A trichothiodystrophy. Nat. Struct. Mol. Biol. **15:**980–984.
23. **Kaldis, P., A. A. Russo, H. S. Chou, N. P. Pavletich, and M. J. Solomon.** 1998. Human and yeast cdk-activating kinases (CAKs) display distinct substrate specificities. Mol. Biol. Cell **9:**2545–2560.
24. **Kraemer, K. H., D. D. Levy, C. N. Parris, E. M. Gozukara, S. Moriwaki, S. Adelberg, and M. M. Seidman.** 1994. Xeroderma pigmentosum and related disorders: examining the linkage between defective DNA repair and cancer. J. Investig. Dermatol. **103**:96S–101S.
25. **Lafforet, D., and J. M. Dupuy.** 1978. Photosensibilite et reparation de l'ADN. Arch. Franc. Pediat. **35:**65–74.
26. **Lehmann, A. R.** 2003. DNA repair-deficient diseases, xeroderma pigmentosum, Cockayne syndrome and trichothiodystrophy. Biochimie **85:**1101–1111.
27. **Luijsterburg, M. S., et al.** 2010. Stochastic and reversible assembly of a multiprotein DNA repair complex ensures accurate target site recognition and efficient repair. J. Cell Biol. **189:**445–463.
28. **Mathieu, N., N. Kaczmarek, and H. Naegeli.** 2010. Strand- and site-specific DNA lesion demarcation by the xeroderma pigmentosum group D helicase. Proc. Natl. Acad. Sci. U. S. A. **107:**17545–17550.
29. **Mitchell, D. L., C. A. Haipek, and J. M. Clarkson.** 1985. (6-4)Photoproducts are removed from the DNA of UV-irradiated mammalian cells more efficiently than cyclobutane pyrimidine dimers. Mutat. Res. **143:**109–112.
30. **Moser, J., et al.** 2007. Sealing of chromosomal DNA nicks during nucleotide excision repair requires XRCC1 and DNA ligase III alpha in a cell-cycle-specific manner. Mol. Cell **27:**311–323.
31. **Nishiwaki, Y., et al.** 2004. Trichothiodystrophy fibroblasts are deficient in the repair of UV-induced cyclobutane pyrimidine dimers and (6-4)photoproducts. J. Investig. Dermatol. **122:**526–532.
32. **Nouspikel, T.** 2009. DNA repair in mammalian cells: nucleotide excision repair: variations on versatility. Cell. Mol. Life Sci. **66:**994–1009.
33. **O'Donovan, A., A. A. Davies, J. G. Moggs, S. C. West, and R. D. Wood.** 1994. XPG endonuclease makes the 3′ incision in human DNA nucleotide excision repair. Nature **371:**432–435.
34. **Ogi, T., et al.** 2010. Three DNA polymerases, recruited by different mechanisms, carry out NER repair synthesis in human cells. Mol. Cell **37:**714–727.
35. **Ranish, J. A., et al.** 2004. Identification of TFB5, a new component of general transcription and DNA repair factor IIH. Nat. Genet. **36:**707–713.
36. **Riou, L., et al.** 1999. The relative expression of mutated XPB genes results in xeroderma pigmentosum/Cockayne's syndrome or trichothiodystrophy cellular phenotypes. Hum. Mol. Genet. **8:**1125–1133.
37. **Roza, L., et al.** 1990. Effects of microinjected photoreactivating enzyme on thymine dimer removal and DNA repair synthesis in normal human and xeroderma pigmentosum fibroblasts. Cancer Res. **50:**1905–1910.
38. **Sijbers, A. M., et al.** 1996. Xeroderma pigmentosum group F caused by a defect in a structure-specific DNA repair endonuclease. Cell **86:**811–822.
39. **Staresincic, L., et al.** 2009. Coordination of dual incision and repair synthesis in human nucleotide excision repair. EMBO J. **28:**1111–1120.
40. **Stefanini, M., et al.** 1993. Genetic heterogeneity of the excision repair defect associated with trichothiodystrophy. Carcinogenesis **14:**1101–1105.
41. **Stefanini, M., G. Orecchia, G. Rabbiosi, and F. Nuzzo.** 1986. Altered cellular response to UV irradiation in a patient affected by premature ageing. Hum. Genet. **73:**189–192.
42. **Stefanini, M., et al.** 1993. A new nucleotide-excision-repair gene associated with the disorder trichothiodystrophy. Am. J. Hum. Genet. **53:**817–821.
43. **Sugasawa, K.** 2010. Regulation of damage recognition in mammalian global genomic nucleotide excision repair. Mutat. Res. **685:**29–37.
44. **Sugasawa, K., J. Akagi, R. Nishi, S. Iwai, and F. Hanaoka.** 2009. Two-step recognition of DNA damage for mammalian nucleotide excision repair: directional binding of the XPC complex and DNA strand scanning. Mol. Cell **36:**642–653.
45. **Sugasawa, K., et al.** 1998. Xeroderma pigmentosum group C protein complex is the initiator of global genome nucleotide excision repair. Mol. Cell **2:**223–232.
46. **Tirode, F., D. Busso, F. Coin, and J. M. Egly.** 1999. Reconstitution of the transcription factor TFIIH: assignment of functions for the three enzymatic subunits, XPB, XPD, and cdk7. Mol. Cell **3:**87–95.
47. **Vandenberghe, K., I. Casteels, E. Vandenbussche, F. De Zegher, and K. De Boeck.** 2001. Bilateral cataract and high myopia in a child with trichothiodystrophy: a case report. Bull. Soc. Belge Ophtalmol. **2001:**15–18.
48. **van der Spek, P. J., et al.** 1996. XPC and human homologs of RAD23: intracellular localization and relationship to other nucleotide excision repair complexes. Nucleic Acids Res. **24:**2551–2559.
49. **van Hoffen, A., J. Venema, R. Meschini, A. A. van Zeeland, and L. H. Mullenders.** 1995. Transcription-coupled repair removes both cyclobutane pyrimidine dimers and 6-4 photoproducts with equal efficiency and in a sequential way from transcribed DNA in xeroderma pigmentosum group C fibroblasts. EMBO J. **14:**360–367.
50. **van Vuuren, A. J., et al.** 1993. Evidence for a repair enzyme complex involving ERCC1 and complementing activities of ERCC4, ERCC11 and xeroderma pigmentosum group F. EMBO J. **12:**3693–3701.
51. **Vermeulen, W., et al.** 2000. Sublimiting concentration of TFIIH transcription/DNA repair factor causes TTD-A trichothiodystrophy disorder. Nat. Genet. **26:**307–313.
52. **Vermeulen, W., P. Osseweijer, A. J. de Jonge, and J. H. Hoeijmakers.** 1986. Transient correction of excision repair defects in fibroblasts of 9 xeroderma pigmentosum complementation groups by microinjection of crude human cell extracts. Mutat. Res. **165:**199–206.
53. **Vermeulen, W., et al.** 1994. Clinical heterogeneity within xeroderma pigmentosum associated with mutations in the DNA repair and transcription gene ERCC3. Am. J. Hum. Genet. **54:**191–200.
54. **Vermeulen, W., M. Stefanini, S. Giliani, J. H. Hoeijmakers, and D. Bootsma.** 1991. Xeroderma pigmentosum complementation group H falls into complementation group D. Mutat. Res. **255:**201–208.
55. **Vermeulen, W., et al.** 1994. Three unusual repair deficiencies associated with transcription factor BTF2(TFIIH): evidence for the existence of a transcription syndrome. Cold Spring Harbor Symp. Quant. Biol. **59:**317–329.
56. **Vitorino, M., et al.** 2007. Solution structure and self-association properties of the p8 TFIIH subunit responsible for trichothiodystrophy. J. Mol. Biol. **368:**473–480.
57. **Volker, M., et al.** 2001. Sequential assembly of the nucleotide excision repair factors in vivo. Mol. Cell **8:**213–224.
58. **Weeda, G., et al.** 1997. A mutation in the XPB/ERCC3 DNA repair transcription gene, associated with trichothiodystrophy. Am. J. Hum. Genet. **60:**320–329.
59. **Yokoi, M., et al.** 2000. The xeroderma pigmentosum group C protein complex XPC-HR23B plays an important role in the recruitment of transcription factor IIH to damaged DNA. J. Biol. Chem. **275:**9870–9875.
60. **Zhou, Y., H. Kou, and Z. Wang.** 2007. Tfb5 interacts with Tfb2 and facilitates nucleotide excision repair in yeast. Nucleic Acids Res. **35:**861–871.
61. **Zotter, A., et al.** 2006. Recruitment of the nucleotide excision repair endonuclease XPG to sites of UV-induced DNA damage depends on functional TFIIH. Mol. Cell. Biol. **26:**8868–8879.
62. **Zurita, M., and C. Merino.** 2003. The transcriptional complexity of the TFIIH complex. Trends Genet. **19:**578–584.